MCR Lab, Department of Geography, University of Basel, Basel, Switzerland

Vertical Structure of Selected Turbulence Characteristics above an Urban Canopy

C. Feigenwinter, R. Vogt, and **E. Parlow**

Summary

In this paper the results of an urban measurement campaign are presented. The experiment took place from July 1995 to February 1996 in Basel, Switzerland. A total of more than 2000 undisturbed 30-minute runs of simultaneous measurements of the fluctuations of the wind vector u', v', w' and the sonic temperature θ_s' at three different heights ($z = 36$, 50 and 76 m a.g.l.) are analysed with respect to the integral statistics and their spectral behaviour. Estimates of the zero plane displacement height d calculated by the temperature variance method yield a value of 22 m for the two lower levels, which corresponds to 0.92 h (the mean height of the roughness elements). At all three measurement heights the dimensionless standard deviation σ_w/u_* is systematically smaller than the Monin-Obukhov similarity function for the inertial sublayer, however, deviations are smaller compared to other urban turbulence studies. The σ_θ/θ_* values follow the inertial sublayer prediction very close for the two lowest levels, while at the uppermost level significant deviations are observed. Profiles of normalized velocity and temperature variances show a clear dependence on stability. The profile of friction velocity u_* is similar to the profiles reported in other urban studies with a maximum around $z/h = 2.1$. Spectral characteristics of the wind components in general show a clear dependence on stability and dimensionless measurement height z/h with a shift of the spectral peak to lower frequencies as thermal stability changes from stable to unstable conditions and as z/h decreases. Velocity spectra follow the $-2/3$ slope in the inertial subrange region and the ratios of spectral energy densities $S_w(f)/S_u(f)$ approach the value of 4/3 required for local isotropy in the inertial subrange. Velocity spectra and spectral peaks fit best to the well established surface layer spectra from Kaimal et al. (1972) at the uppermost level at $z/h = 3.2$.

1. Introduction

It is a well known problem, that methods for estimating the turbulent exchange, which were developed for rather smooth, homogeneous surfaces, actually can not be transferred to the urban boundary layer, where the surface is rough and inhomogeneous. In spite of that, due to a lack of better knowledge, the semi-empirical methods of the Monin-Obukhov similarity (MOS) theory are still used in flow and diffusion modelling (Beniston, 1987; Frenzen et al., 1987; Gross, 1989; Gryning and Lyck, 1984; Hanna and Chang, 1992), though its validity must be questioned.

The urban boundary layer can be divided into a roughness sublayer (RS) close to the roughness elements, followed by the inertial sublayer (IS) and topped by the (convective) mixed layer (ML) (Raupach et al., 1991). The RS and the IS together are also known as the surface layer. The RS extends up to 2–5 times the height of the roughness element h. The air flow in this layer is three dimensional due to the strong influences of the local building structures. Higher up in the IS the influences of a larger area are mixed in such a

way, that the turbulent characteristics in the IS represent an area of average roughness. The well founded MOS relations can be applied to describe the turbulent fluxes and statistics in the IS, and therefore, the exchange of momentum, heat and mass can be calculated.

A first and often used approach to the problem is to investigate and to describe the deviations of the turbulent and spectral characteristics from their "ideal" values. Few studies deal with observations of the turbulence structure of the air flow over built-up areas. One of the assumptions made in MOS theory is, that the turbulent fluxes are constant with height. This is obviously not the case in the present study. So if i.e. the friction velocity u_* is not constant with height, the Monin-Obukhov length L also becomes essentially local and so does in consequence the stability parameter z/L. Similarly, the flux of sensible heat is found to be non-constant with height. Also the profiles of momentum flux and sensible heat flux observed at the present site depend strongly on stability. As a possible solution of the problem, the concept of local scaling is applied. Högström et al. (1982) and Rotach (1993b) found the concept of local scaling (local momentum flux values are used for normalization) to be valid for the description of velocity variances and wind-shear within the upper part of the urban roughness sublayer. However, the normalized standard deviations of vertical wind velocity are systematically smaller compared to MOS prediction as also is reported by Clarke et al. (1982), Rotach (1991) and Roth and Oke (1993b). Rotach (1993a) and Oikawa and Meng (1995) found similar profiles of u_*, which show a maximum at the supposed border between the RS and the IS. Despite the inhomogeneity and the roughness of an urban surface, Roth and Oke (1993a) reported spectral/cospectral characteristics which differed only slightly to data from the homogeneous surface layer.

The aim of this campaign was to provide a reliable dataset to investigate the vertical structure of turbulence and organized motion above an urban canopy. The whole data set is analysed within the Monin-Obukhov similarity framework. Nondimensionalized and spectral properties of the turbulent flow are compared to standard surface layer relationships, and espe- cially the dependence of the observed relations of height and stability is investigated and discussed.

2. Experimental Setup and Data Processing

The data analysed in this paper were collected during a special measurement campaign as a part of the BASTA-project (BAsler STAdtklima) from July 1995 to February 1996 in the inner city of Basel, Switzerland. In order to extend the probing of the urban boundary layer above the roughness sublayer, turbulence instrumentation was mounted on a 50 m antenna tower, which has its basement at 24 m above street level. The tower has a triangle cross section with a sidelength of 1.25 m at the bottom and 0.5 m at the top. Within 500 m around the tower, the percentage of area covered by buildings over total area is ≈50% and the average building height is ≈24 m.

Three ultrasonic anemometer-thermometers (sonics) measured at three heights the fluctuations of the wind vector (u', v', w') and the sonic temperature (θ'_s). At the two lower levels, the sonics were mounted at the end of a horizontal 6 m boom, at the uppermost level, the instrument was mounted right on the top. The data were sampled at 20.83 Hz and all raw data were stored for subsequent analysis. Additionally two profiles of wind speed (u), and one profile of air temperature (θ) and humidity (q) were measured, each profile consisting of six heights. Wind direction (α) was determined at three levels, and net radiation (R_n) was measured at 64 m. The profile data were stored as 10 min averages on a data logger (Campbell 21X). See Table 1 and Fig. 1 for an overview of the experimental setup.

The raw data of each sonic were sampled via serial port and stored as transit counts on three PCs, which have been synchronized for time at least once within three days. Maximum deviations were in the range of ±1.25 seconds per day. The raw data were scaled using a matrix calibration derived from wind tunnel experiments (Vogt, 1995). All three sonics were recalibrated after the measurement campaign in a wind tunnel in March 1996 and were also intercompared during a field campaign in April 1996 (Vogt et al., 1997). To minimize tower effects and to prevent for flow distortion by sonic geometry only data from an undistributed wind sector ($224° < \alpha$

Table 1. *Instrumental Setup (see also Fig. 1)*

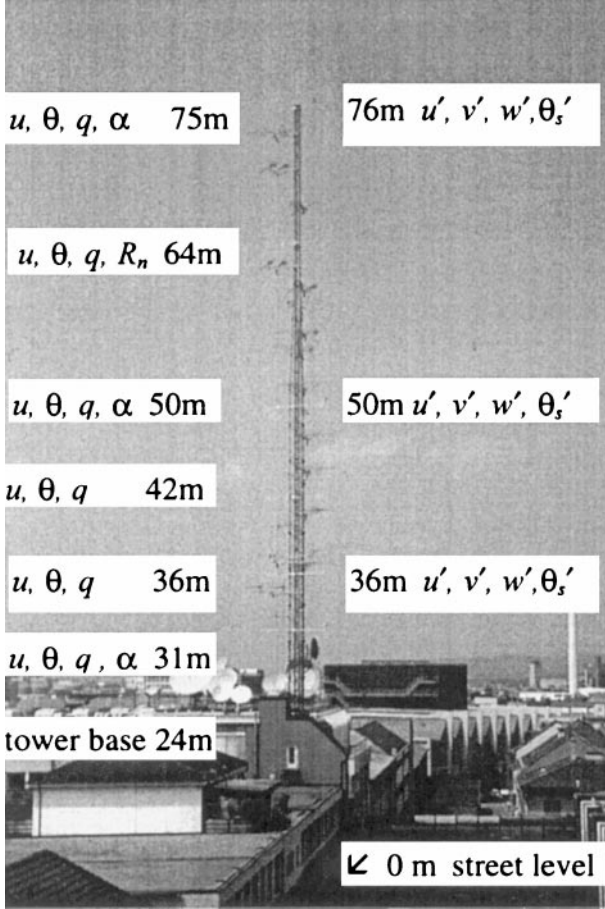| Variable	Instrument	Manufacturer	Height [m] a.g.l.
u	cup anemometer	Vaisala WAA15	75, 64, 50, 42, 36, 31
u, α	propeller vane	Young	75, 50, 36
θ, q	thermistor, capacitive sensor	Vaisala HMP35A in ventilated radiation shield	75, 64, 50, 42, 36, 31
R_n	pyrradiometer	Schenk Mod. 8111	64
u', v', w', θ_s'	ultrasonic anemometer thermometer	Gill-Solent, R2, asymmetric head	76, 50, 36

Fig. 1. The measurement tower in the inner city of Basel, Switzerland. For instruments setup refer to Table 1

$< 103°$) were selected for the analysis. Additionally, runs with mean wind speeds lower than $2\,\mathrm{ms}^{-1}$ at the uppermost measurement level were not included in the analysis. This resulted in a total of more than 1000 analysed 53-minute runs (2^{16} samples) for the spectral characteristics and more than 2000 30-minute runs for the analysis of the integral statistics and profiles (see also Table 4).

3. Results and Discussion

3.1 Zero Plane Displacement Height

The zero plane displacement height d was determined by the temperature variance method described in Rotach (1994). Under certain conditions the surface of a city can be regarded as thermally homogeneous, even though it is dynamically rough. Therefore the measurement of the dimensionless temperature variance σ_θ/θ_* can be used for the determination of d providing that the same d is valid for the flux of momentum as well as for the flux of latent heat. According to MOS theory the following function describes the behaviour of σ_θ/θ_* for unstable conditions in the SL (from de Bruin et al., 1993; after Wyngaard et al., 1971; and Tillmann, 1972):

$$\frac{\sigma_\theta}{\theta_*} = -C_1 \left(1 - C_2 \frac{z - d}{L} \right)^{-\frac{1}{3}}, \qquad (1)$$

where θ_* denotes the temperature scale ($\theta_* = -\overline{w'\theta'}/u_*$), L the Monin-Obukhov length, and the constants C_1 and C_2 are 2.9 and 28.4.

To get an estimate of d, the difference between measured and calculated values is minimized according to Eq. (2) by varying d.

$$err = \left(\frac{1}{N} \sum_{i=1}^{N} \left(\frac{\sigma_{\theta_i}}{\theta_{*i}} - \left(\frac{\sigma_\theta}{\theta_*} \right)_{i(1)} \right)^2 \right)^{\frac{1}{2}} \qquad (2)$$

In Eq. (2), N is the number of measurements and *err* is the value to be minimized.

Table 2 gives an overview on the results of the temperature variance method for the undisturbed sector of wind direction. The resulting averaged d estimates for the lower two measurement heights are 21 m and 23.5 m correspond quite well whereas at the topmost level we find an unrealistic high value of about 40 m. The reason

Table 2. *Values for the Zero Plane Displacement Height d Calculated by the Temperature Variance Method for the Selected Wind Direction Sectors* (number of runs per sector in brackets)

Height	Azimuth								Average
	$240°\pm15°$	$270°\pm15°$	$300°\pm15°$	$330°\pm15°$	$0°\pm15°$	$30°\pm15°$	$60°\pm15°$	$90°\pm15°$	$225°-105°$
$z/h = 3.2$	47.0 (12)	42.0 (68)	39.0 (26)	39.0 (99)	37.0 (50)	35.0 (2)	34.0 (4)	48.0 (51)	**40.1**
$z/h = 2.1$	29.5 (15)	23.5 (115)	26.5 (39)	22.5 (106)	19.5 (47)	–	19.5 (5)	23.5 (53)	**23.5**
$z/h = 1.5$	25.5 (18)	22.0 (120)	22.0 (47)	20.0 (125)	19.0 (54)	18.5 (3)	24.5 (3)	16.5 (56)	**21.0**

for this could be the different source area of this sensor that probably does not fullfill the conditions for thermal homogeneity. A zero plane displacement of 22 m corresponds to 0.92 times the building height h, which seems comparatively high to values for vegetation canopies, which are in the range of 2/3 to 3/4 h. However, considering that urban buildings stand very close together and are stiff compared to a vegetation canopy, so that the wind profile can not penetrate very deep into the urban canopy, and also taking into account the excellent agreement of the results from the lower two sonics, it is justified to use a d-value of 22 m for all further calculations.

3.2 Integral Statistics and Profiles

3.2.1 Profiles of Velocity and Temperature Standard Deviations and Friction Velocity

In Figs. 2, 3 and 4 average profiles of velocity and temperature standard deviations are shown for the four stability classes stable ($z/L > 0.05$), neutral ($-0.05 \leq z/L \leq 0.05$), slightly unstable ($-0.5 \leq z/L \leq -0.05$) and unstable ($z/L \leq -0.05$). Standard deviations σ_u, σ_v and σ_w and the friction velocity u_* are scaled with the u_*-value from the uppermost measurement level at $z/h = 3.2$ and error bars indicate the run-to-run variability. In the near neutral case profiles of σ_u and σ_v in Fig. 2a and 2b are nearly uniform, whereas σ_w increases slightly with height. Taking into account the small scatter, the values correspond surprisingly well to the recommended values of 2.4, 1.9 and 1.25 by Panofsky and Dutton (1984) for σ_u/u_*, σ_v/u_* and σ_w/u_*, respectively, for neutral conditions and flat terrain. Under unstable conditions the profiles of σ_u and σ_v decrease with height, whereas for stable conditions σ_u increases and σ_v has a relative

Fig. 2. Scaled profiles of standard deviations of wind components a) $\sigma_u/u_{*\text{top}}$ b) $\sigma_v/u_{*\text{top}}$ and c) $\sigma_w/u_{*\text{top}}$

minimum at $z/h = 2.1$. The scaled vertical velocity variance σ_w shows an increase with height from neutral to unstable conditions, differences become larger as instability increases. This is in contrast to the observation of Rotach (1995), who reported a decrease of σ_w with increasing height for near-neutral stratifications.
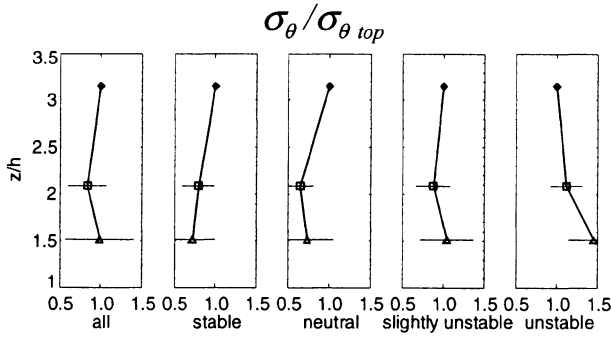
Fig. 3. Scaled profiles of standard deviations of temperature

The profile of temperature variance normalized by the σ_θ value of the uppermost level (Fig. 3) shows a strong decrease of σ_θ with increasing height for unstable conditions. At $z/h = 1.5$ fluctuations are about 50% higher than at $z/h = 3.2$. For stable and neutral stratifications, σ_θ is reduced in the lower levels compared to the top level. This increase of σ_θ between $z/h = 2.1$ and $z/h = 3.2$ for slightly unstable to stable stratifications supports the idea of different thermal source areas, as we would expect σ_θ to decrease with height.

Profiles of friction velocity u_* are displayed in Fig. 4. For unstable stratification u_* decreases slightly between the two upper levels, whereas for the remaining cases, a significant increase with height between the two lower levels can be observed. Under stable stratification the maximum occurs at $z/h = 2.1$ at the second measurement level. Considering these profiles and taking into account Rotach's (1993a) suggestion to consider the RS as the layer within u_* increases from zero to the IS value, we can set the upper boundary of the RS somewhere around the second measurement level at $z/h = 2.1$. A similar
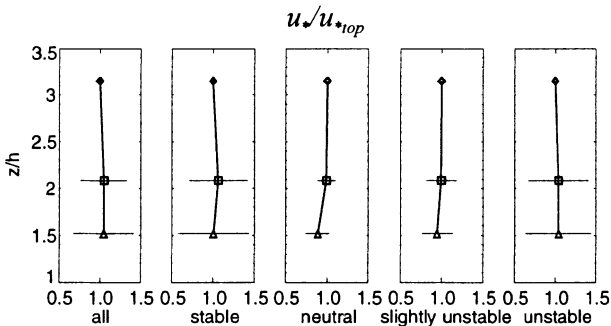

Fig. 4. Scaled profiles of friction velocity u_*

profile of u_* is reported in Oikawa and Meng (1995).

3.2.2 Normalized Standard Deviations

The analysis shows that the dimensionless standard deviation for the vertical wind velocity σ_w/u_* is systematically smaller for all three measurement heights than the values predicted by the MOS function for σ_w/u_* for "ideal" surfaces:

$$\frac{\sigma_w}{u_*} = C_1 \left(1 - C_2 \frac{z-d}{L} \right)^{\frac{1}{3}}. \qquad (3)$$

The coefficients C_1 and C_2 in Eq. (3) are taken from Panofsky and Dutton (1984) as 1.25 and 3. A similar behaviour is reported by Clarke et al. (1982), Roth and Oke (1993b), Rotach (1993b) and Oikawa and Meng (1995), however, deviations to the reference in our study are smaller, which is shown in Fig. 5 left. Note that local values of u_* and L are taken. As listed in Table 3, all urban studies report smaller values for C_1 and C_2 in Eq. (3), therefore, one can conclude that over rough urban surfaces an enhanced mechanical production of vertical velocity fluctuations is established.

Since the zero plane displacement height d was determined by the temperature variance method (see previous section), the σ_θ/θ_* values are practically forced to follow the MOS function in Eq. (1). This works quite well for the two lower levels, however, the large anomalies at the uppermost level at $z/h = 3.2$ in Fig. 5 right suggests, that thermal homogeneity is not given for the source area of this sensor. This is also in agreement to the statement derived from the σ_θ-profile in Fig. 3 in the previous section and the failure of the temperature variance method for this measurement level.

3.3 Spectral Characteristics

Time series of 53 minutes (2^{16} samples) have been chosen for spectral analysis. Before calculating the spectra, data were corrected for possible non-stationarities by linear detrending and tapered with a cosine taper prior to the discrete Fourier transformation (Stull, 1988; Kaimal and Finnigan, 1994).
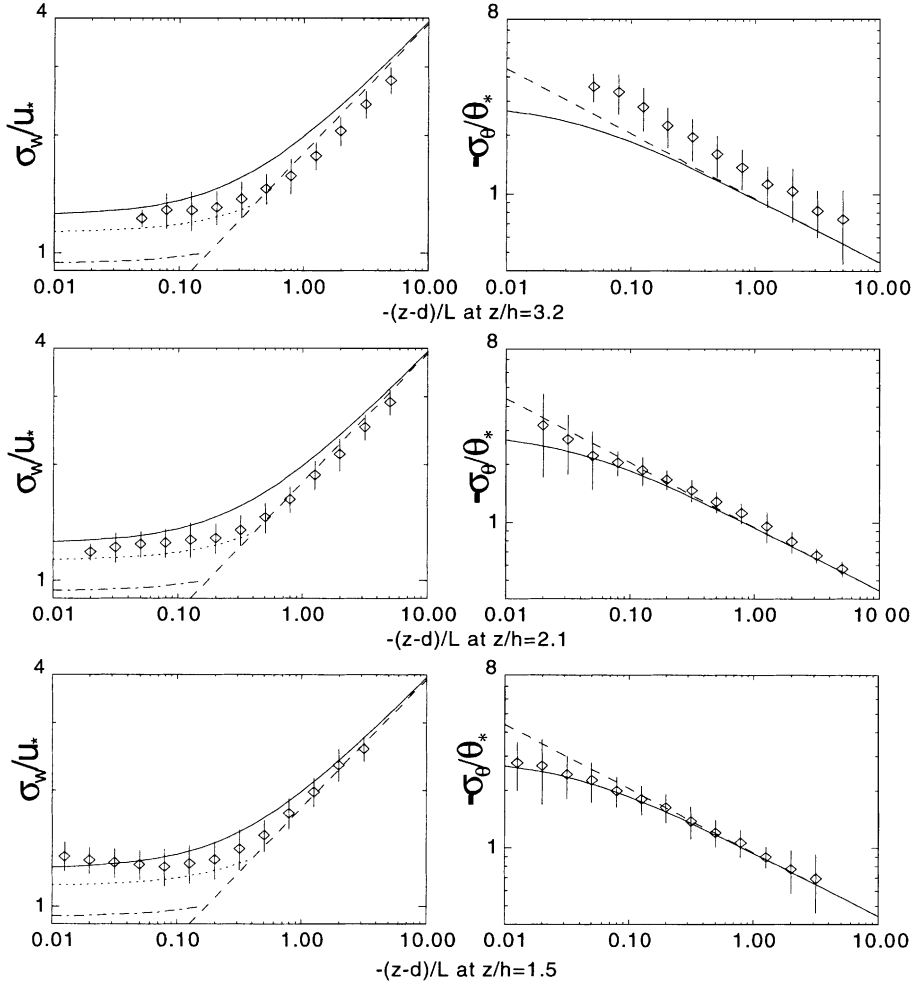
Fig. 5. Left column: σ_w/u_* values for unstable conditions. Plotted are class averages with one standard deviation as error bar. Functional relationships are from Panofsky and Dutton (1984) (solid), Clarke et al. (1982) (dotted) and Rotach (1993b) (dashed-dotted). Right column: same as left, but for σ_θ/θ_*. Functional relationship is after de Bruin et al. (1993) (solid). The free convection limit is indicated by the dashed line

Table 3. *Comparison of Values C_1 and C_2 in Eq. (3) from Different Studies*

C_1	C_2	z/h	surface	study
1.25	3		"ideal"	Panofsky and Dutton (1984)
1.13	1.56	$z/h \approx 4$	average value of four urban sites, $0 \geq z/L \geq -5$	Clarke et al. (1982)
0.94	1.29	$1.27 \leq z/h \leq 1.55$	urban site, $0 \geq z/L \geq -1$	Rotach (1993b)
1.16	2.36	$z/h = 3.2$	urban site, $-0.02 \geq z/L \geq -8$	this study
1.14	2.82	$z/h = 2.1$		
1.18	2.95	$z/h = 1.5$		

The presented spectra and cospectra are normalized by their respective variances and covariances and plotted against the non-dimensional frequency $f = n(z - d)/\bar{u}$, where n denotes the natural frequency in Hz and $\bar{u}$ the mean wind speed over the sampling time. The averaged mean wind speed over all runs was 3.9 m/s at the uppermost level. Note that all spectra and frequencies are normalized by their local values. All single spectra were fitted by a cubic spline and then averaged into the four stability classes. The number of runs per class are listed in Table 4. Spectral and cospectral peak frequencies are compared in Table 5 and Table 6 to other urban turbulence studies.

Additionally the well established Kansas spectra from Kaimal et al. (1972) for neutral conditions are plotted in the following figures for

Table 4. *Stability Classes and Number of 53-minute Runs for Composite Spectra Calculation*

z/h	Stable $z/L>0.05$	Neutral $-0.05\leq z/L\leq0.05$	Weakly unstable $-0.5\leq z/L<-0.05$	Unstable $z/L<-0.5$
1.5	63	386	709	147
2.1	79	244	702	280
3.2	173	164	511	455

Table 5. *Spectral Peak Frequencies of Wind Components u, v and w above Urban Surfaces (Except Kaimal et al., 1972) from Various Studies*

Study	Peak frequency			Height z/h	Stability
	u	v	w		
Kaimal et al. (1972)	0.045	0.142	0.45		neutral
Rotach (1995)	0.1..1.2		≈0.65	1.55	$0>z/L>-1$
	0.05..0.5		≈1.4	1.27	$0>z/L>-1$
Högström et al. (1982)	5.053 ± 0.017	0.24 ± 0.037	0.54 ± 0.12	3.5	$-0.2<z/L<0.2$
	0.101 ± 0.039	0.11 ± 0.02	0.35 ± 0.08	1.3	$-0.2<z/L<0.2$
Oikawa and Meng (1995)	0.02..0.05		0.1..0.4	2.5	$-0.08>z/L>-0.23$
Roth and Oke (1993a)	≈0.02	≈0.14	≈0.15	2.65	$-0.05>z/L>-1.8$
This study	≈0.044	≈0.131	≈0.38	3.2	$-0.05>z/L>-0.5$
	≈0.029	≈0.085	≈0.31	2.1	$-0.05>z/L>-0.5$
	≈0.015	≈0.044	≈0.25	1.5	$-0.05>z/L>-0.5$

Table 6. *(Co)Spectral Peak Frequencies of Temperature θ, Momentum Flux $\overline{u'w'}$ and Kinematic Heat Flux $\overline{w'\theta'}$ above Urban Surfaces (except Kaimal et al., 1972) from Various Studies*

Study	Peak frequency			Height z/h	Stability
	θ	$u'w'$	$w'\theta'$		
Kaimal et al. (1972)	0.063	0.07	0.09		neutral
Rotach (1991, 1995)	distorted	≈0.25	≈0.25	1.55	$-0>z/L>-1$
Roth and Oke (1993a)	≈0.04	≈0.035	≈0.045	2.65	$-0.05>z/L-1.8$
This study	distorted	≈0.085	≈0.16	3.2	$-0.05>z/L-0.5$
	≈0.085	≈0.044	≈0.085	2.1	$-0.05>z/L>-0.5$
	≈0.068	≈0.055	≈0.085	1.5	$-0.05>z/L>-0.5$

comparison reasons. Note that the velocity spectra are scaled with the variance whereas the Kansas spectra scale with u_*, this explains the differences in the power level. The slopes of $-2/3$ and $-4/3$ in the following figures indicate the proportionality of the spectral and cospectral energy densities, respectively, to the inertial subrange laws predicted by Kolmogorov's hypothesis.

3.3.1 Velocity Spectra

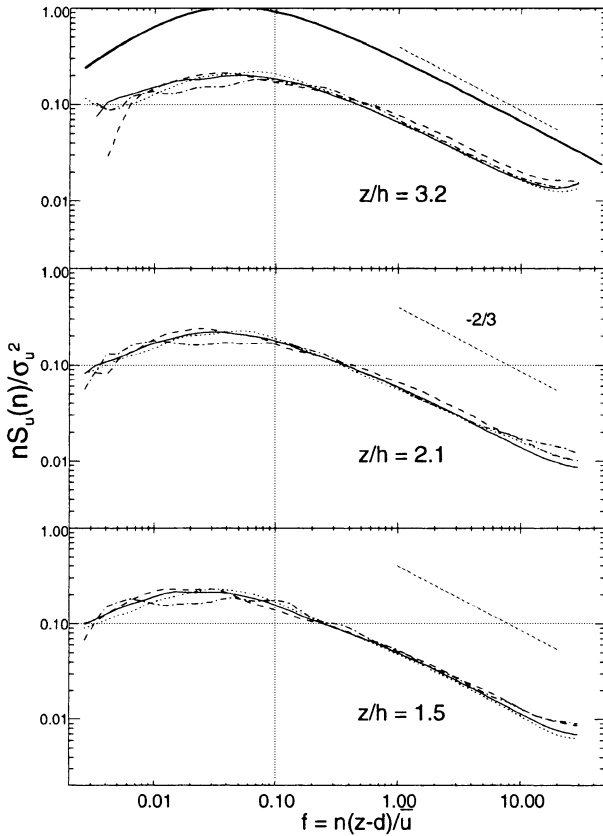In Figs. 6, 7 and 8 the composite spectra of the wind components u, v and w are shown for all

Fig. 6. Spectra of longitudinal wind component u for stable (dashed-dotted), neutral (dotted), weakly unstable (solid) and unstable (dashed) conditions. Reference spectrum from Kaimal et al. (1972) (solid thick)

Fig. 7. As Fig. 6 but for lateral wind component v

three measurement heights and the four stability classes. In the inertial subrange they all follow the $-2/3$ slope. In contrast to the lateral and vertical velocity spectra, the spectra of the longitudinal velocity u in Fig. 6 do not exhibit a strong stability dependence. Only a weak tendency for a peak shift to lower frequencies can be observed at each height as stratification becomes more unstable. Spectral peaks for weakly unstable conditions occur in then region of $f_m \approx 0.044$ for $z/h = 3.2$ and shift to lower frequencies for all stability classes as we come closer to the roughness elements. Since $f_m = (z-d)/\lambda_m$ by virtue of Taylor's hypothesis, the dominant eddy scale or peak wavelength λ_m for the longitudinal component u ranges from 1200 m at $z/h = 3.2$ to 969 m at $z/h = 2.1$ and 960 m at $z/h = 1.5$ for weakly unstable conditions.

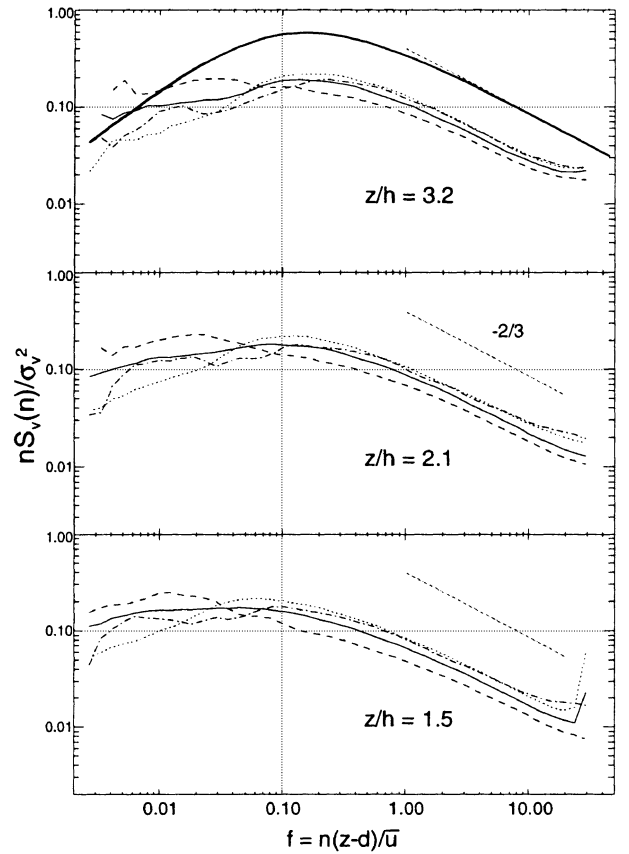The spectra of the lateral and vertical wind components v and w in Figs. 7 and 8 show a clear stability dependence at all three measurement heights. Spectral energy densities for unstable conditions are significantly higher in the low frequency range and the spectral peaks are shifted to lower frequencies as instability increases. In the inertial subrange, the $-2/3$ slope is well established, but in contrast to the longitudinal wind component spectral densities in the inertial subrange are lowest for unstable conditions and they increase as stratification becomes more and more stable. As observed with the u-spectra, the peak frequencies of the v- and w-spectra shift to lower values as z/h decreases. Peak frequencies f_m of w-spectra in the weakly unstable case are 0.38, 0.31 and 0.25 from top to bottom. This corresponds to dominant eddy scales λ_m of 141 m, 91 m and 58 m.

Since the peak wavelengths λ_m decrease for all three wind components as we approach the surface from the uppermost measurement level, the dimensions of the dominant eddy structures
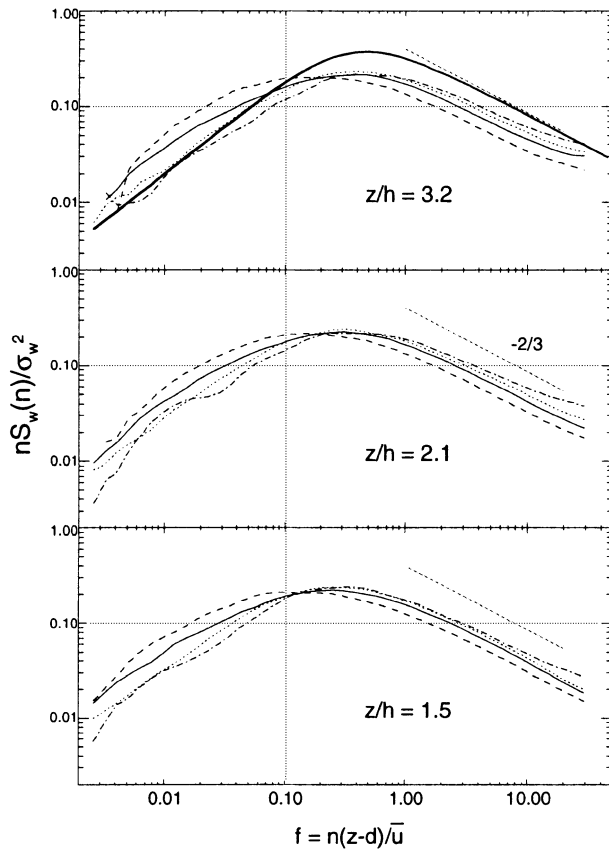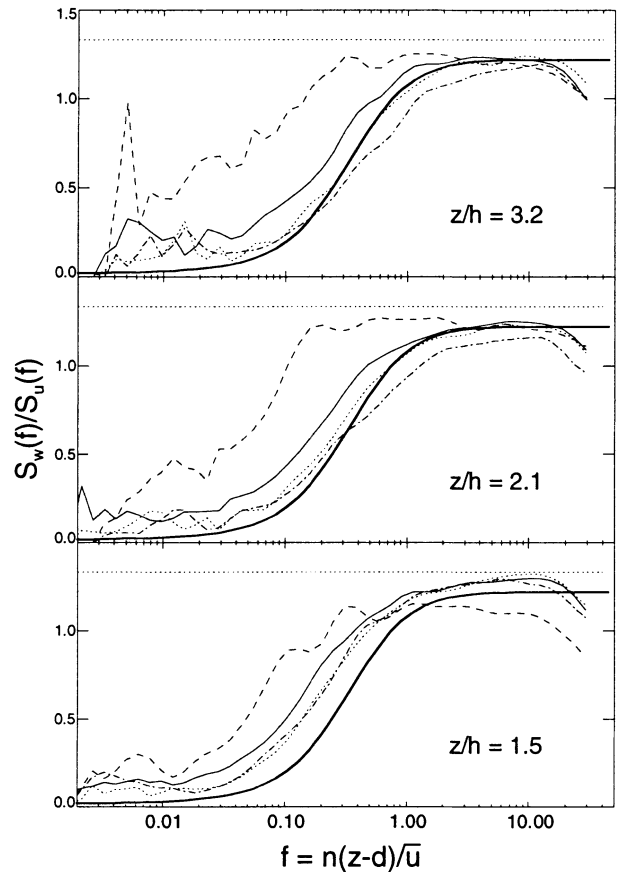
Fig. 8. As Fig. 6 but for vertical wind component w

Fig. 9. As Fig. 6 but for ratios of spectral energy densities $S_w(f)/(S)_u(f)$. Reference curve solid thick from Kaimal et al. (1972)

become smaller. The peak frequencies of the surface layer reference spectra from Kaimal et al. (1972) fit best to the uppermost level at $z/h = 3.2$ for all three wind components, which suggests that this measurement level is above the roughness sublayer within the inertial sublayer. In Table 5 the observed spectral peak spectral peak frequencies of wind components are compared to values reported in other urban studies. The scatter between the values for the same variable in quite large, but one has to consider the different measurement heights and the different "urban" surfaces. Roth and Oke (1993a) and Oikawa and Meng (1995) measured over relatively uniform suburban areas (mean building height $h = 8.5\,\mathrm{m}$ and $7\,\mathrm{m}$, respectively) with a percentage of area covered by buildings of about 25%, while Högström et al. (1982) and Rotach (1995) were investigating european cities ($h = 15\,\mathrm{m}$ and $20\,\mathrm{m}$, respectively) with about 50% of total area covered by buildings, which is

similar to the present study. Additionally the number of runs analysed in the study is significantly larger in all studies mentioned above (see Table 4).

Horizontal and vertical velocity composite spectra exhibit the predicted $-2/3$ slope at the high frequency range and therefore, one could conclude, that an inertial subrange is observed within the urban roughness sublayer. As an additional test based on Kolmogorov's hypothesis concerning local isotropy in this frequency range, the ratio of the vertical to the longitudinal spectral energy densities $S_w(f)/S_u(f)$ is expected to approach 4/3. This ratio is drawn in Fig. 9 for all measurement heights and stability classes. Note that the Kansas spectra are not adjusted to provide the 4/3 ratio (Kaimal and Finnigan, 1994). This is in good agreement with the $z/h = 3.2$ level, however the $z/h = 1.5$ curve approaches the 4/3 line best. Rotach (1995) reported values for $S_w(f)/S_u(f)$ smaller than 1

at $z/h = 1.55$ and concluded that there is no inertial subrange within the urban roughness sublayer. However the present data and the values from Högström et al. (1982), who reported $S_w(f)/S_u(f)$ ratios of 1.3 and 1.06 for $z/h = 3.5$ and $z/h = 1.3$, respectively, suggest that an inertial subrange is established.

3.3.2 Temperature Spectra

Temperature spectra in Fig. 10 are generally ill-defined and flat for stable and neutral conditions at all heights and also for weakly unstable conditions at $z/h = 3.2$. The increase of the spectral densities at the low frequency end of these spectra indicate a significant mesoscale component, which is also observed by Clarke et al. (1982). Rotach (1995) explains the higher spectral densities at low frequencies with warm bubbles rising sporadically from the street canyon. The fact that the increase of spectral densities at the low frequency end is most pronounced at the uppermost level supports the

idea of a different thermal regime at the uppermost measurement level as supposed in a previous section, though the interpretation of temperature spectra must be made with caution. A striking feature of all temperature spectra is their increase at the high frequency end at all heights and a stabilities at $f > 5$, which might reflect a noisy signal. The $-2/3$ slope in the inertial subrange is only followed for unstable conditions, the corresponding peak frequencies are 0.085, 0.069 and 0.044 for $z/h = 3.2$, 2.1 and 1.5, respectively.

3.3.3 Cospectra

As for temperature spectra there are not many studies that deal with cospectra over urban surfaces. Some of the few are compared to this study in Table 5. Because of the larger scatter and occasional negative values, the curve for stable conditions are not well formed, nevertheless they are plotted in Fig. 11, too. Cospectra of $u'w'$ are well established for neutral and
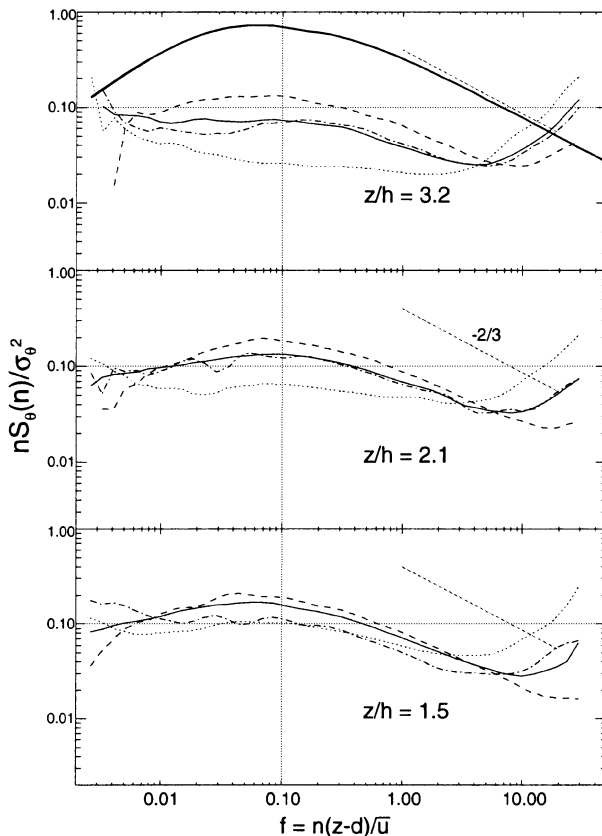

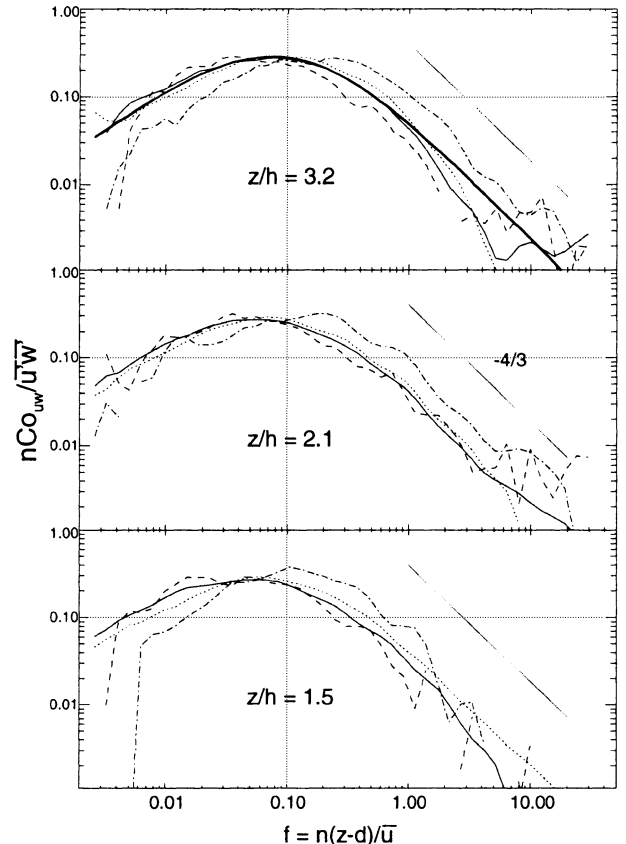Fig. 10. As Fig. 6 but for sonic temperature θ_s

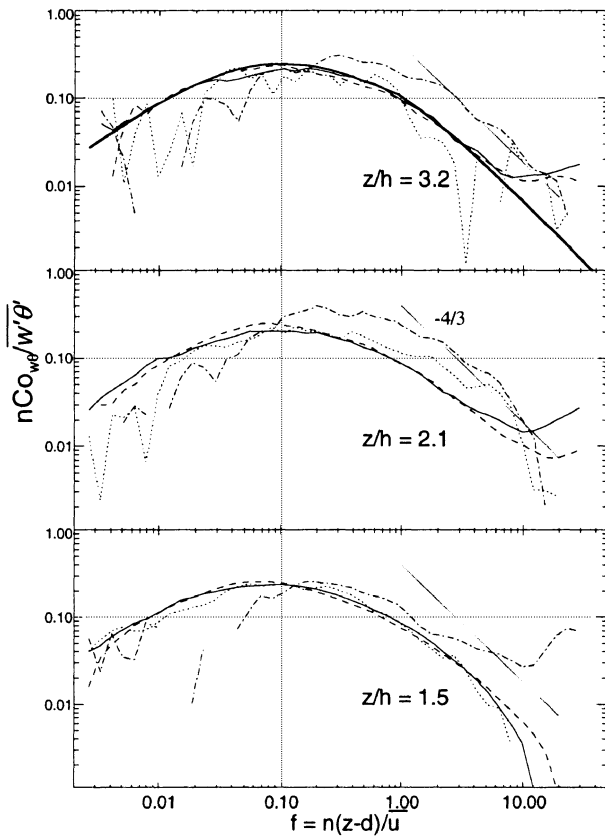Fig. 11. As Fig. 6 but for Cospectra of $u'w'$

Fig. 12. As Fig. 6 but for Cospectra of $w'\theta'$

weakly unstable conditions, however the $-4/3$ slope is not given for the uppermost level in the inertial subrange and peak locations for the two lower levels are slightly shifted to lower values (Table 6). Cospectra of $w'\theta'$ in Fig. 12 behave very similar to those of $u'w'$, again the curves are not well defined at all measurement levels for the stable stability class and at $z/h = 3.2$ and $z/h = 2.1$ for the neutral class. Nevertheless the reference cospectrum agrees almost perfectly in shape and peak frequency with the weakly unstable cospectra of the two lower levels, whereas the peak frequency for $z/h = 3.2$ is shifted to a higher value of $f_m \approx 0.16$. Compared to the velocity spectra, cospectra do not show that distinct height and stability dependence, what makes a clear interpretation difficult.

4. Summary and Conclusions

Simultaneously measured turbulent time series at three different heights ($z/h = 1.5$, 2.1 and 3.2)

above an urban canopy in Basel, Switzerland, were analysed within the Monin-Obukhov similarity framework and with respect to their spectral characteristics. Results are compared to previous studies made over urban surfaces.

1) Both σ_w/u_* and σ_θ/θ_* follow the predicted $(-)1/3$ power law dependence for free-convection. The normalized standard deviation σ_w/u_* for unstable conditions is found to be systematically smaller at all three measurement heights than rural reference data, but larger than the values from comparable studies over urban surfaces (Clarke et al., 1982; Rotach, 1993b).

2) Scaled average profiles of standard deviations of the horizontal velocity components σ_u and σ_v, and of temperature σ_θ show a clear stability dependence such as a decrease with height under unstable conditions and an increase with height under stable conditions. The standard deviation of the vertical component σ_w is found to generally increase with height and differences become larger as instability increases.

3) The profiles of friction velocity u_* are found to decrease continuously with height only under unstable conditions, whereas under weakly unstable to stable conditions u_* shows a maximum at $z/h = 2.1$. This seems to be characteristic for the urban roughness sublayer, as similar profiles are reported by Rotach (1993a) and Oikawa and Meng (1995).

4) Spectral peaks of wind component u, v and w show a clear height dependence such as a shift to higher frequencies as height increases. The predicted $-2/3$ slope in the inertial subrange region is generally well established and the ratio S_w/S_u approaches a value of 1.22 at $z/h = 2.1$. and 1.3 at $z/h = 1.5$. This leads to the conclusion, that an inertial subrange is established though we are in the urban roughness sublayer. Peak frequencies fit best to the Kansas reference spectra at the uppermost measurement level at $z/h = 3.2$, but are slightly lower. The spectra of v and w show an obvious shift to lower frequencies as instability increases, whereas the u-spectra show only a weak stability dependence.

5) Temperature spectra and cospectra of $w'\theta'$ are generally not well defined for stable and neutral stratifications. At the uppermost measurement level at $z/h = 3.2$ temperature spectra are very flat also for weakly unstable and unstable conditions and do not show a distinct peak.

6) Three facts suggests that the uppermost level at $z/h = 3.2$ is probably ruled by another turbulent thermal regime than the two lower levels, namely: a) the failure of the temperature variance method for the determination of the zero plane displacement d, b) the significant deviation from MOS prediction for σ_θ/θ_*, and c) the flat and ill-defined temperature spectra.

Mechanical properties in the urban roughness sublayer such as profiles of velocity variances, non-dimensionalized velocity variances and spectra of wind componnents behave similar to rural reference data and other urban studies. They ar parametrized quite well within the MOS framework, if local scaling is applied. Parametrization of thermal properties in the urban roughness sublayer and inertial sublayer within the MOS framework however is not satisfactory, since different measurement levels show different behaviour to standard equations probably due to thermal inhomogeneity and/or different source areas.

Since this is first study that describes the vertical dependence of velocity spectra in the urban surface layer by the analysis of a large number of runs, there is certainly a need for more experiments in this field to confirm the results of this and previous studies. Thereby it should also to be taken in account that the structure of urban surfaces depends heavily on regional aspects, e.g. they are not of the same kind in Europe and in North America.

Acknowledgements

References

Beniston, M., 1987: A numerical study of atmospheric pollution over complex terrain in Switzerland. *Bound.-Layer Meteor.,* **41**, 75–96.

Clarke, J. F., Ching, J. K. S., Godowich, J. M., 1982: A study of turbulence in a urban environment. EPA 600-53-82-062, EPA.

De Bruin, H. A. R., Koshiek, W., van den Hurk, B. J. J. M., 1993: A verification of some methods to determine the fluxes of momentum, sensible heat and water vapour using standard deviation and structure parameter of scalar meteorological quantities. *Bound.-Layer Meteor.,* **63**, 231–257.

Frenzen, G., Heimann, D., Wamser, M., 1987: Dokumentation des Regionalen Klimamodells (RKM) auf der Basis von FITNAH. DFVLR-Mitt. 87–07.

Gross, G., 1989: Numerical simulation of the nocturnal flow systems in the Freiburg area for different topographies. *Beiträge zur Physik der Atmosphäre,* **62**, 57–72.

Gryning, S.-E., Lyck, E., 1984: Atmospheric dispersion from elevated sources in an urban area: comparison between tracer experiments and model calculations. *J. Climate Appl. Meteor.,* **23**, 651–660.

Hanna, S. R., Chang, J. C., 1992: Boundary-Layer parametrizations for applied dispersion modeling over urban areas. *Bound.-Layer Meteor.,* **58**, 229–259.

Högström, U., Bergström, H., Alexandersson, H., 1982: Turbulence characteristics in a near neutrally stratified urban atmosphere. *Bound.-Layer Meteor.,* **23**, 449–472.

Kaimal, J. C., Wyngaard, J. C., Izumi, J., Coté, O. R., 1972: Spectral characteristics of surface-layer turbulence. *Quart. J. Roy. Meteor. Soc.,* **98**, 563–589.

Kaimal, J. C., Finnigan, J. J., 1994: *Atmospheric Boundary Layer Flows: Their Structure and Measurement.* New York: Oxford University Press, 289 pp.

Oikawa, S., Meng, Y., 1995: Turbulence characteristics and organized motions in a suburban roughness sublayer. *Bound.-Layer Meteor.,* **74**, 289–312.

Panofsky, H. A., Dutton, J. A., 1984: *Atmospheric Turbulence. Models and Methods for Engineering Applications.* New York: John Wiley & Sons, 397 pp.

Rotach, M. W., 1991: *Turbulence within and above an Urban Canopy.* ETH Diss. 9439, published as *ZGS,* Heft 45, Zürich: Verlag GGIETH, 240 pp.

Rotach, M. W., 1993a: Turbulence close to a rough urban surface. Part I: Reynolds stress. *Bound.-Layer Meteor.,* **65**, 1–28.

Rotach, M. W., 1993b: Turbulence close to a rough urban surface. Part II: Variances and gradients. *Bound.-Layer Meteor.,* **66**, 75–92.

Rotach, M. W., 1994: Determination of the zero plane displacement in an urban environment. *Bound.-Layer Meteor.,* **67**, 187–193.

Rotach, M. W., 1995: Profiles of turbulence statistics in and above an urban street canyon. *Atmos. Environ.,* **29**, 1473–1486.

Roth, M., Oke, T. R., 1993a: Tubulent transfer relationships over an urban surface: I: Spectral characteristics. *Quart. J. Roy. Meteor. Soc.,* **119**, 1071–1104.

Roth, M., Oke, T. R., 1993b: Tubulent transfer relationships over an urban surface: II: Integral statistics. *Quart. J. Roy. Meteor. Soc.,* **119**, 1105–1120.

Stull, R. B., 1988: *An Introduction to Boundary Layer Meteorology.* Dordrecht: Kluwer Academic Publishers, 666 pp.

Tillmann, J. E., 1972: The indirect determination of stability, heat and momentum fluxes in the atmospheric boundary

layer from simple scalar variables during dry unstable conditions. *J. Appl. Meteor.,* **11**, 783–792.

Vogt, R., 1995: Theorie, Technik and Analyse der experimentellen Flussbestimmung am Beispiel des Hartheimer Kiefernwaldes. Ein Beitrag zu den Energiebilanzuntersuchungen im REKLIP, *stratus 3,* Diss. Phil-. Nat. -Fak. Univ. Basel, Basel, 101 pp.

Vogt, R., Feigenwinter, C., Paw U. K. T., Pitacco, A., 1997: Intercomparison of ultrasonic anemometers, *Preprints of the 12th Symposium of Boundary Layers and Turbulence,* Vancouver, Canada. Am. Met. Soc., 354–355.

Wang, J., 1992: Turbulence characteristics in an urban atmosphere of complex terrain. *Atmos. Environ.,* **25A**, 2717–2724.

Wyngaard, J. C., Coté, O. R., Izumi, Y., 1971: Local free convection, similarity, and the budgets of shear stress and heat flux. *J. Atmos. Sci.,* **28**, 1171–1182.

Authors' addresses: Dipl. Geogr. Christian Feigenwinter, Dr. Roland Vogt, and Prof. Dr. Eberhard Parlow, MCR Lab, Department of Geography, University of Basel, Spalenring 145, CH-4055 Basel, Switzerland.